

International Atomic Energy Agency

INDC(CPR)-021
Distr.: L

INDC

INTERNATIONAL NUCLEAR DATA COMMITTEE

X-RAY ATTENUATION COEFFICIENTS AND PHOTOELECTRIC
CROSS SECTIONS OF Cu, Fe AND Sn FOR THE ENERGY RANGE 3-29 KeV

Wang Dachun, Yang Hua, Luo Pingan, Ding Xunliang,
Wang Xinfu, Zhou Hongyu, Shen Xinyin and Zhu Guanghua
Beijing Radiation Center
Institute of Low Energy Nuclear Physics
Beijing Normal University
Beijing, China

July 1991

IAEA NUCLEAR DATA SECTION, WAGRAMERSTRASSE 5, A-1400 VIENNA

X-RAY ATTENUATION COEFFICIENTS AND PHOTOELECTRIC
CROSS SECTIONS OF Cu, Fe AND Sn FOR THE ENERGY RANGE 3-29 KeV

Wang Dachun, Yang Hua, Luo Pingan, Ding Xunliang,
Wang Xinfu, Zhou Hongyu, Shen Xinyin and Zhu Guanghua
Beijing Radiation Center
Institute of Low Energy Nuclear Physics
Beijing Normal University
Beijing, China

July 1991

Reproduced by the IAEA in Austria
August 1991

91-03138

Contents

X-Ray Attenuation Coefficients and Photoelectric Cross Sections of Sn for the Energy Range 3.3 KeV to 29.1 KeV By Wang Dachun, Yang Hua and Luo Pingan	5
X-Ray Attenuation Coefficients and Photoelectric Cross Sections of Cu and Fe for the Range 3 KeV to 29 KeV By Wang Dachun, Ding Xunliang, Wang Xinfu, Yang Hua, Zhou Hongyu, Shen Xinyin and Zhu Guanghua	11

X-RAY ATTENUATION COEFFICIENTS AND PHOTOELECTRIC CROSS
SECTIONS OF Sn FOR THE ENERGY RANGE 3.3 KeV TO 29.1 KeV *

Wang Dachun Yang Hua Luo Pingan

(Beijing Radiation Center)

(Institute of Low Energy Nuclear Physics, Beijing Normal University)

ABSTRACT

Using a new type X-ray source produced by proton excitation of elementary or compound targets and Si(Li) detector system, mass attenuation coefficients of tin have been determined for the energy range from 3.3 to 29.1 KeV. The experimental uncertainties of attenuation coefficients have been reduced to $\pm 1\%$ for intenser isolated characteristic X-rays. The total photoelectric cross sections have been obtained by subtracting scattering cross sections from the measured total cross sections.

1. Introduction

Tin is an important metal material in common use. The X-ray attenuation coefficients and photoelectric cross sections of Tin are important atomic data and interest both in the fundamental physics and many applied fields. In the past a number of scientists had measured such data at the similar X-ray energy range to ours [1-20]. However the deviations among different results were larger. At some energy points the maximum deviations exceeded $\pm 15\%$. The more accurate experimental values of the X-ray attenuation coefficients and photoelectric cross sections for Sn are needed. That is not only for comparison with and checking of the theoretical calculation, but also for analytical works and other applied fields which make use of X rays.

Using a new type X-ray source [21] which produced by means of proton beam of Tandem accelerator to bombard elementary targets, high-energy resolution Si(Li) detector and the technique of computer processing spectrum, the accuracies of experimental data have been improved to $\pm 1 - \pm 2\%$. We selected 35 characteristic lines of 12 elements and systematically measured the attenuation coefficients of Sn. For the intenser isolated characteristic X rays, the experimental uncertainty of attenuation coefficients have been reduced to $\pm 1\%$. The photoelectric cross sections were determined by subtracting the contribution of the coherent and the incoherent scattering from the measured total cross sections. Comparison of the present experimental results with the past values, as well as between the experimental data and theoretical calculations, have been presented and discussed.

2. Experimental Method

In this work we measured the total attenuation cross sections with the transmission technique on a "narrow-beam geometry" setup. Experimental targets, including KCl, Ti, V, Fe, Ni, Cu, Nb, Mo, Ag, Sn, Y, Pb, etc., were prepared by vacuum vaporization method. The purities of target materials are better than 99.98%. The range of targets thickness is about 0.3 - 1.5 mg/cm². The tin absorbers were prepared by means of rolling press or vacuum vaporization. The range of area thickness of absorber foils is from 0.5 to 100 mg/cm². The average area thickness of absorber foil and the uniformity of experimental foils can be guaranteed to be less than $\pm 0.5\%$. The purities of Sn absorber foil is 99.99%.

* This work were supported by International Atomic Energy Agency and Union of atomic and molecular data research of China.

9 X ray spectra were measured with and without an absorber foil placed in the centre of X-ray collimator system yielding the transmitted and the original photon intensities. For most of absorbers enough counts were accumulated to make the uncertainty due to counting statistics to be much less than $\pm 1\%$. The attenuation coefficient μ (in cm^2/g) can be obtained by fitting experimental data with the least-squares method and the following equation :

$$\ln I(t) = \ln I(0) - \mu t \quad (1)$$

where $I(t)$ and $I(0)$ is the normalized photon intensity with and without the absorber foil respectively, t is the absorber foil thickness in g/cm^2 . More than 5 absorber foils with different thickness in the range of $2 < I(0)/I(t) < 55$ were selected for each energy point.

The total attenuation cross sections σ_{tot} were calculated from the following expression:

$$\sigma_{\text{tot}} = 10^{24} \mu A/N \quad (\text{b/atom}) \quad (2)$$

where A is the atomic mass of Sn element, N is Avogadro's number. σ_{tot} is in unit of barns/atom. The photoelectric cross section σ_{ph} is obtained from σ_{tot} by subtracting the coherent and the incoherent scattering cross sections as interpolated from the tabulation value of J.H.Hubbell et al.[22][23].

3. Results and Discussions

Mass attenuation coefficients of Sn measured at 35 characteristic line energies of 12 elements have been arranged in Table 1. Because of Si(Li) detector resolution has limited,utilizing AXIL program of computer analysis for spectrum, only K_{α} , K_{β} lines were represented for Ti, V, Fe, Ni, Cu elementary targets and K_{α} , $K_{\beta_{13}}$ and K_{β_2} lines of Nb, Mo, Ag, Y and Sn elementary targets were extracted. The experimental spectra of Pb were dissolved into $L_{\alpha_{12}}$, $L_{\beta_{123}}$, L_{γ_1} , L_{γ_2} , L_{γ_3} etc. lines by Gaussian least-squares fit. The present experimental result of mass attenuation coefficient for Sn and the partial earlier experimental results are shown in Fig.1 and Table 1. The solid line in Fig.1 is the polynomial least-squares-fitted line with present results.

The fitting of the X-ray mass attenuation coefficient of Sn at the energy range between 4.5 KeV and 28.5 KeV was obtained by

a third degree polynomial of the form:

$$Y = A_0 + A_1 \cdot X + A_2 \cdot X^2 + A_3 \cdot X^3 \quad (3)$$

where

$$Y = \ln \mu,$$

$$X = \ln E_x,$$

E_x is the x-ray energy in KeV. The fitting coefficients are as follows:

$$\begin{aligned} A_0 &= 0.990861 \text{ E}+01 \\ A_1 &= -0.119941 \text{ E}+01 \\ A_2 &= -0.574203 \text{ E}+00 \\ A_3 &= 0.710388 \text{ E}-01 \end{aligned}$$

TABLE 1. The experimental results for Sn

Target	Transition	Energy (KeV)	μ (cm^2/g)	σ_{tot} (b/atom)	σ_{ph} (b/atom)
KCL	K_{α}	3.313	491.2 \pm 4.9	9.6811E04	9.5640E04
	K_{β}	3.590	390.1 \pm 3.9	7.6885E04	7.5755E04
Ti	K_{α}	4.509	1142.0 \pm 11.4	2.2508E05	2.2407E05
	K_{β}	4.932	913.3 \pm 9.2	1.8000E05	1.7905E05
V	K_{α}	4.950	900.9 \pm 9.0	1.7756E05	1.7661E05
	K_{β}	5.427	708.0 \pm 7.1	1.3954E05	1.3865E05
Fe	K_{α}	6.399	478.3 \pm 4.8	9.4268E04	9.3476E04
	K_{β}	7.058	368.5 \pm 3.7	7.2628E04	7.1896E04
Ni	K_{α}	7.472	315.1 \pm 3.2	6.2103E04	6.1406E04
	K_{β}	8.265	243.2 \pm 2.4	4.7932E04	4.7295E04

TABLE 1. (Continue)

Target	Transition	Energy (KeV)	μ (cm ² /g)	σ_{tot} (b/atom)	σ_{ph} (b/atom)
Cu	K α	8.041	271.2 \pm 2.7	5.3451E04	5.2798E04
	K β	8.905	199.6 \pm 2.0	3.9339E04	3.8745E04
Y	K α	14.931	47.56 \pm 0.48	9.3736E03	9.0149E03
	K β_{13}	16.734	36.09 \pm 0.36	7.1130E03	6.7935E03
	K β_2	17.015	34.82 \pm 0.56	6.8627E03	6.5487E03
Nb	K α	16.583	35.91 \pm 0.36	7.0775E03	6.7550E03
	K β_{13}	18.617	26.28 \pm 0.27	5.1795E03	4.8955E03
	K β_2	18.953	25.36 \pm 0.55	4.9982E03	4.7202E03
Mo	K α	17.443	32.21 \pm 0.32	6.3483E03	6.0426E03
	K β_{13}	19.603	22.95 \pm 0.23	4.5232E03	4.2564E03
	K β_2	19.965	22.09 \pm 0.37	4.3537E03	4.0931E03
Ag	K α	22.103	16.63 \pm 0.17	3.2776E03	3.0509E03
	K β_{13}	24.932	11.92 \pm 0.12	2.3493E03	2.1598E03
	K β_2	25.456	11.04 \pm 0.25	2.1759E03	1.9920E03
Sn	K α	25.192	11.45 \pm 0.12	2.2567E03	2.0700E03
	K β_{13}	28.472	8.32 \pm 0.09	1.6398E03	1.4785E03
	K β_2	29.109	8.73 \pm 0.36	1.7206E03	1.5620E03
Pb	L β	9.185	186.4 \pm 3.9	3.6738E04	3.6160E04
	L α_{12}	10.542	122.5 \pm 1.2	2.4144E04	2.3639E04
	L η	11.349	99.79 \pm 2.0	1.9668E04	1.9198E04

TABLE 1. (Continue)

Target	Transition	Energy (KeV)	μ (cm ² /g)	σ_{tot} (b/atom)	σ_{ph} (b/atom)
Pb	L β_6	12.143	83.88 \pm 1.7	1.6532E04	1.6092E04
	L β_{123}	12.621	75.07 \pm 0.78	1.4796E04	1.4372E04
	L β_5	13.015	66.97 \pm 0.72	1.3199E04	1.2789E04
	L γ_1	14.764	47.77 \pm 0.49	9.4150E03	9.0523E03
	L γ_{23}	15.165	44.76 \pm 0.56	8.8217E03	8.4685E03

The uncertainties for the attenuation experiment consisted of following terms : (1) The statistical uncertainty of count. (2) The error of measurement for absorption foil thickness and its uniformity . Both were less than $\pm 0.5\%$. (3) The uncertainty of computer dissolving spectrum and background . (4) the effect of scattering photon in solid angle subtended by detector. In our collimator condition the maximal scatter angle was less than 3° . The correction due to the scattering photon can be negligible. For the K α , K β , L α_{12} , L β_{123} , L γ_1 lines of each elementary target the statistical uncertainties of count and the uncertainties due to computer dissolving spectrum and background each and all were less than $\pm 0.5\%$. The total error of mass attenuation coefficients were less than 1% and we set them to be $\pm 1.0\%$. However for some weaker K β_2 and L α lines the statistical uncertainties of count were somewhat greater $\pm 1\%$ and for some superimposed L α peak, the uncertainty of computer dissolving spectrum was one of main error in the final result, the total error of mass attenuation coefficients were greater $\pm 1\%$. These data are also listed to Table 1 and Fig.1 for reference only.

The partial data have been compared with the earlier experimental results and shown in Fig.1 and Table 2. It is obvious that the present results are agreement with the average of the earlier results. The total photoelectric cross sections σ_{ph} (in b/atom), obtained by subtracting scattering cross section from the measured total cross sections, are listed to Table 1. The fitting of the photoelectric cross sections for the energy range between 4.5 KeV and 28.5 KeV have been obtained by a third degree

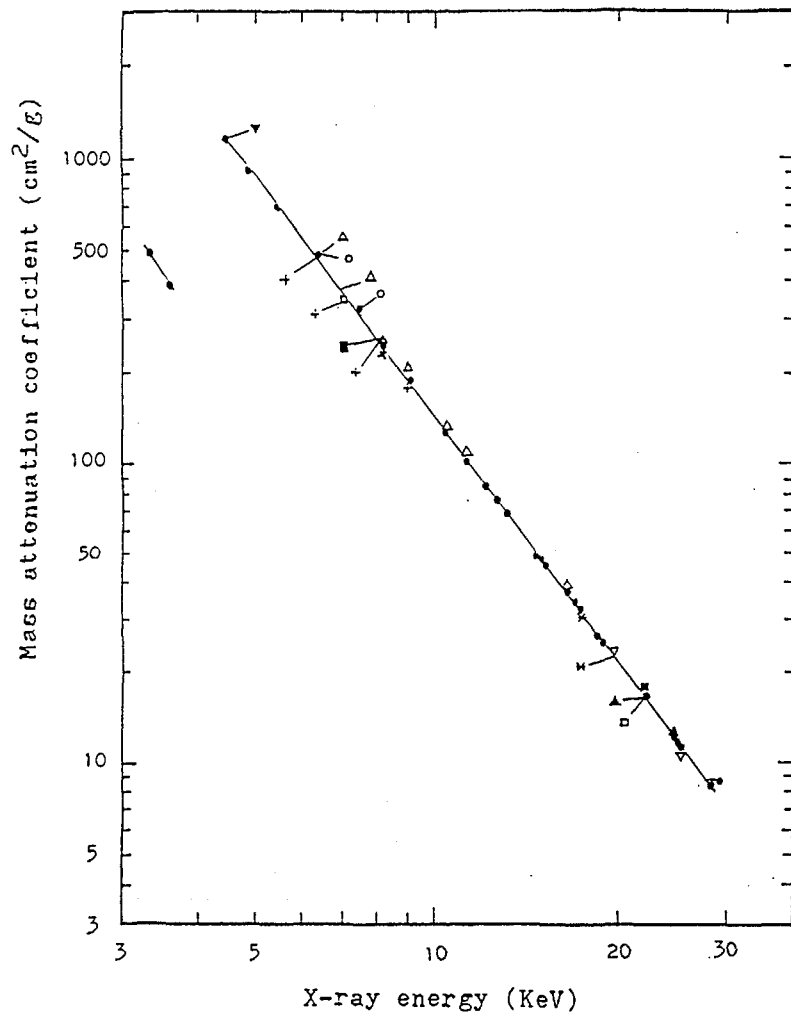


FIG. 1 Comparison of experimental results of mass attenuation coefficient for Sn
 • present work, ○ BA[1], □ BA[2], ■ BR[3],
 △ AL[6], ▽ MA[10], ▲ NO[12], × BE[13],
 + PA[18], * MA[19]

TABLE 2. Comparison of experimental results for Sn

X-ray energy (KeV)	Mass attenuation coefficient (in cm ² /g)							
	Present	BA[1]	BA[2]	AL[6]	MA[10]	NO[12]	BE[13]	PA[18]
4.509	1142					1121.3		
6.399	478.3	479.7	472	490				472.4
7.058	368.5		328	385				336.9
7.472	315.1	326.2		325				
8.041	271.2	272.9	272	275			252.7	249.6
8.905	199.6			205				179.1
10.542	122.5			132				
11.349	99.79			110				
16.583	35.91			39.0		WI[4]	RI[7]	MA[19]
17.443	32.21			32.5	32.6	35.04	31.5	30.1
19.603	22.95	BR[3]			23.5	AL[5]		22.4
22.103	16.63	17.96	16.5		17.5	16.5		
24.932	11.92	12.08			11.9	12.8		
25.192	11.45				10.2			
28.472	8.32				8.7			

TABLE 3. Comparison of photoelectric cross sections (in b/atom) for Sn with theoretical values of Scofield [24]

Energy (KeV)	Present	Scofield	Deviation
4.472	0.2284E+6	0.2184E+6	+4.6 %
5.000	0.1735E+6	0.1661E+6	+4.5 %
6.000	0.1093E+6	0.1035E+6	+5.6 %
8.000	0.5117E+5	0.4864E+5	+5.2 %
10.000	0.2786E+5	0.2675E+5	+4.1 %
15.000	0.8990E+4	0.8835E+4	+1.8 %
20.000	0.3996E+4	0.3971E+4	+0.6 %
29.156	0.1392E+4	0.1374E+4	+1.3 %

polynomial of form:

$$Z=B_0+B_1 \cdot X+B_2 \cdot X^2+B_3 \cdot X^3 \quad (4)$$

where

$$Z=\ln \sigma_{ph.}$$

$$X=\ln E_x.$$

The fitting coefficients are as follows:

$$B_0= 0.150960E+02$$

$$B_1=-0.109676E+01$$

$$B_2=-0.606124E+00$$

$$B_3= 0.699940E-01$$

The total photoelectric cross sections were compared with the theoretical compilations of Scofield [24] in Table 3. At X-ray energy range of 3 to 29 KeV photoeffect is a most essential interaction process. The total contribution of coherent and incoherent scattering is less than 11 % and the uncertainty of scattering cross section can not obviously influence the error of photoelectric cross sections. The present results of photoelectric cross section are greater than the theoretical values of Scofield [24] to 3.5 % on an average.

Using X rays produced by proton excitation of elementary targets and Si(Li) detector, the signal to noise ratio of characteristic X rays was promoted to 1-2 orders of magnitude in comparison with radioactive X-ray source or X-generator-secondary combination source. At the same time the error of dissolving spectrum was decreased. Experimental uncertainties of attenuation coefficients were reduced to ± 1 % for intense isolated X rays. Consequently, the results would be more confident and reliable than the earlier.

REFERENCES

- [1] Barkla C.G. and Sadler C.A., Philos.Mag., Vol.14, 408(1907)
- [2] Barkla C.G. and Sadler C.A., Philos.Mag., Vol.17, 739(1909)
- [3] Bragg W.H. and Peirce S.E., Philos.Mag. Vol.28, 626(1914)
- [4] Wingardh K. A., Z.Phys. Vol.8, 363(1922)
- [5] Allen S.J.M., Phys.Rev. Vol.27, 266(1925)
- [6] Allen S.J.M., Phys.Rev. Vol.28, 907(1926)
- [7] Richtmyer F.K., Phys.Rev. Vol.27, 1(1926)
- [8] Richtmyer F.K., Phys.Rev. Vol.30, 755(1927)
- [9] Kastner H., Z.Phys. Vol.70, 468(1931)
- [10] Martin L.H. and Lang K.C.
Proc.R.Soc.London, Sect.A137, 199(1932)
- [11] AFOSR-TN-58-784(1958)
- [12] Nordfors B. and Noreland E., Ark.Fys., 20, 1(1961)
- [13] Bearden A.J., J.Appl.Phys. Vol.37, 1681(1966)
- [14] Mccrary J.H. et al., Phys.Rev. Vol.153, 307(1967)
- [15] Knerr R.R. and Vonach, H., Z.Angew.Phys., Vol.22, 507(1967)
- [16] Gharman B.S. and Sood B.S., Curr.Sci. Vol.37, 250(1968)
- [17] Sahota H.S., Indian J.Phys., Vol.46, 526(1972)
- [18] Parthasaradhi K. and Hansen H.H.,
Phys.Rev., A10, 563(1974)
- [19] Manter H., X-ray Spectrometry, Vol.3, 90(1974)
- [20] Puttaswarry K.S. et al., Nuoyd Cimento, A39, 125(1977)
- [21] Ding X.L. and Wang D.C. et al.,
J.Atom. and Mole.Phys.(Chinese), Vol.6, 1085(1989)
- [22] J.H.Hubbell and I.Overbo,
J.Phys. Chem.Ref.Data, Vol.8, 69(1979)
- [23] J.H.Hubbell et al.,
J.Phys.Chem.Ref. Data, Vol.5, 471(1975)
- [24] J.H.Scofield, UCRL - 51326 (1973)

X-RAY ATTENUATION COEFFICIENTS AND PHOTOELECTRIC CROSS SECTIONS

OF Cu AND Fe FOR THE RANGE 3 KeV TO 29 KeV

Wang Dachun Ding Xunliang Wang Xinfu Yang Hua

Zhou Hongyu Shen Xinyin Zhu Guanghua

Beijing Radiation Center (Institute of Low Energy Nuclear

Physics, Beijing Normal University), Beijing, China

ABSTRACT

A new type X-ray source has been obtained by proton excitation of elementary targets or compound targets. Using this X-ray source and Si(Li) detector system mass attenuation coefficients have been determined for copper in the energy range 3.3 - 29.1 KeV, for iron in 3.3-20 KeV. The experimental uncertainties of attenuation coefficients have been reduced to $\pm 1\%$ for intenser isolated characteristic X-rays. The total photoelectric cross sections have been obtained by subtracting scattering cross sections from the measured total cross sections. Comparison of the present experimental results with the past values, as well as between the experimental values and the theoretical calculations, have been presented and discussed.

* This work is supported by International Atomic Energy Agency and Union of atomic and molecular data research of China.

1. Introduction

The X-ray attenuation coefficients are important atomic data and interest both in the fundamental physics and many applied fields. In the past a number of scientists had measured such data of Cu [1-6] and Fe [7-14] at the similar X-ray energy range to ours. However each of them only performed these measurements at a few energy points or even at one energy point. At some energy points the maxium deviations among different results exceeded $\pm 10\%$. The more accurate experimental values for the X-ray attenuation coefficients are needed. That is not only for comparison with and checking of the theoretical calculation, but also for analytical works and other applied fields which make use of X rays.

Copper and Iron are important materials in common use. It is expected to measure the more accurate attenuation cross sections for Cu and Fe. We selected Cu and Fe and measured their attenuation coefficients that is not only to provide more reliable data for practice use, but also to test our X-ray source system, experimental method and setup.

In the present work, a new type X-ray source was obtained by proton excitation of elementary targets. In addition, using high-energy resolution Si(Li) detector and the technique of computer processing spectrum, the accuracies of experimental data can be improved to $\pm 1 - \pm 2\%$. For the intenser isolated characteristic X rays, the experimental uncertainty of attenuation coefficients can be reduced to $\pm 1\%$. The photoelectric cross sections for Cu and Fe have been obtained by subtracting scattering cross sections from the measured total cross sections. Comparison of the present experimental results with the past values, as well as between the experimental values and the theoretical calculations, have been presented and discussed.

2. Experimental Method

The total photoelectric cross sections can be determined by two methods: (1) direct method, measuring the photoelectron or X-ray fluorescence yield under the irradiation of X ray, (2) indirect method, measuring the total attenuation cross sections with the transmission technique on a "good geometry" setup and subtracting the calculated contributions due to the coherent and the incoherent scattering. At low photon energy, photoelectric process is the main interaction process, the coherent and the incoherent scattering processes are very small, therefore, indirect

method is in common use. In the present investigation, we made use of indirect method. The experimental arrangement is shown in Fig.1.

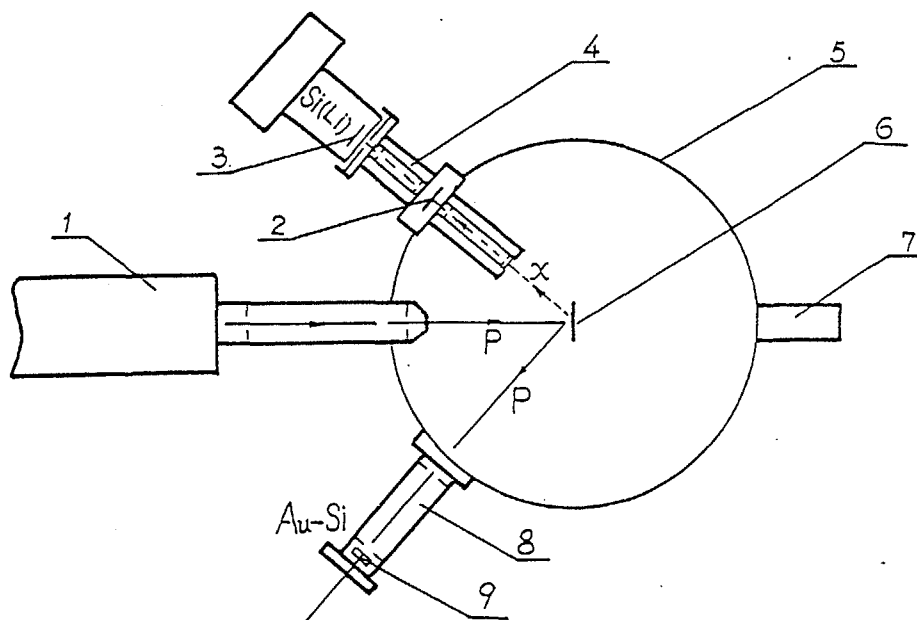


Fig. 1 Experimental arrangement for X-ray attenuation measurements

- | | |
|-------------------------------|--------------------------|
| 1, Accelerator, | 2, Absorbers, |
| 3, Si(Li) detector, | 4, Collimator for X-ray, |
| 5, Vacuum chamber, | 6, Targets, |
| 7, Faraday cup, | |
| 8, Collimator for RBS proton, | 9, Au-Si detector. |

2.5 MeV proton beam of Tandem accelerator past through two apertures with a diameter of 3 mm and bombarded the elementary target without backing at the centre of vacuum chamber so that characteristic X rays were excited. At 135° to the proton beam, X-ray photons transmitting the Mylar window film were collimated by a specially designed collimator and formed a narrow X-ray beam. The narrow X-ray beam perpendicularly passing through the absorbers of Cu or Fe were detected by the Si(Li) detector having a resolution of 170 eV at 6.4 keV. The output pulses from the

detector were amplified and fed to CANBERRA S-35⁺ multichannel analyser and then analysed by IBM-PC microcomputer. At the other side and 135° to the incident proton beam an Au-Si surface barrier detector recorded the proton flux backscattered from the target. The output pulses of Au-Si detector were amplified and counted by a single-channel-analyser-scalar combination. The proton charge past through the target was collected by a Faraday cup and measured by the digital current integrator. The proton charge counts were proportional to the backscattered proton counts within the statistical error. That proved the internal consistency in the two methods of monitoring and normalizing the incident X ray intensity. The proton currents were restricted to 1-50 nA that prevent the pulse pileup of Si(Li) spectrometer system and minimize the dead time correction to the least. The X ray counts were controlled by the live time of multichannel analyser and recorded simultaneously with the monitor counts controlled by timing, consequently, the small dead time correction were automatically carried out.

Experimental targets, including Ti, V, Fe, Ni, Cu, Nb, Mo, Ag, Sn, Pb, Au etc., were prepared by vacuum vaporization method. The purities of target materials were better than 99.98%. The range of targets thickness is about 0.3-1.5 mg/cm².

The absorbers used were prepared by means of rolling press. The range of area thickness of absorber foils is from 0.5 to 40 mg/cm². The foil weight was weighed by microbalance which has accurate to 1 part in 1000000 gram. The area of each foil was carefully measured by a reading microscope which has an amplification of 100 and the accuracy of foil area is better than 0.5%. The average area thickness of absorber foil in unit of mg/cm² was determined by dividing its weight by its area. To ensure a good uniformity of absorber foil, we divided the foil of 5x5 cm² into 9 pieces or cut the foil of 3x5 cm² into 3 parts. If the maximum variance of area thickness of the circumjacent parts was less than $\pm 0.5 - \pm 0.8\%$ the central one was selected as the experimental absorber foil. Hence the uniformity of experimental foils can be guaranteed to be less than $\pm 0.5\%$. The purities of Cu and Fe absorber foils are both 99.99%. These were also proved by the analysis of PIXE and RBS spectra of Cu and Fe foils, therefore the influence of impurity of absorber foil was negligible.

With 2.5 MeV proton beam of Tandem accelerator to bombard elementary targets, the signal to noise ratio of characteristic X rays were measured to be in the range of 70 to 230. The background was mainly due to noise from the detector and the associated electronics. Background spectra were taken in two ways: Firstly, without any target, but with the proton beam on

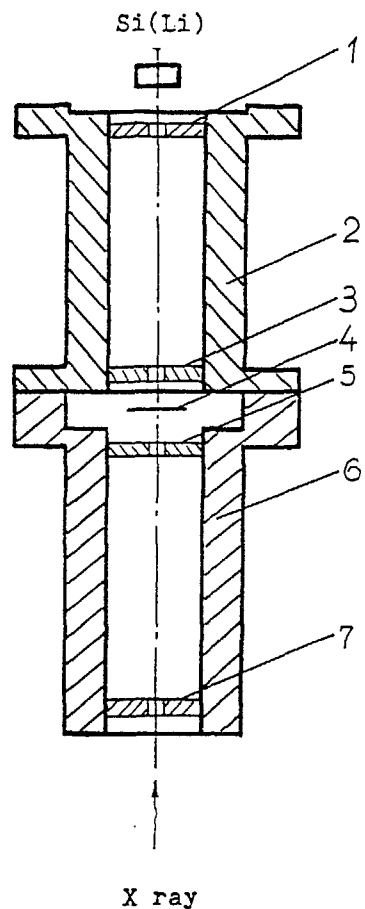


Fig. 2 Scheme of collimator
 1, 3, 5, 7 --- Aperture diaphragm (Al or Pb)
 2, 6 --- Collimator (Al)
 4 --- Absorbers

and secondly, with target and with the proton beam on, but with the incident X-ray channel blocked by a lead block, which completely absorbed the incident X rays. In both cases the background was found to be negligible. The X-ray collimator system, 22 cm in length and having 4 movable collimator apertures, is shown in Fig.2. It provided a narrow-beam geometry for the attenuation measurements. The collimator apertures, made of Al and Pb, can be changed from 3 mm to 8 mm in diameter.

X ray spectra were measured with and without an absorber foil placed in the centre of collimator system yielding the transmitted and the original photon intensities. For most of absorbers enough counts were accumulated to make the uncertainty due to counting statistics to be much less than 1%. The attenuation coefficient can be obtained by fitting experimental data with the least-squares method and the following equation:

$$\ln I(t) = \ln I(0) - \mu t \quad (1)$$

where $I(t)$ and $I(0)$ is the normalized photon intensity with and without the absorber foil respectively, t is the absorber foil thicknesses in g/cm. More than 5 absorber foils with different thickness in the range of $2 < I(0)/I(t) < 55$ were selected for each energy point.

The total attenuation cross sections were calculated from the following expression:

$$\sigma_{\text{tot}} = 10^{24} \mu A/N \text{ (b/atom)} \quad (2)$$

where A is the atomic mass of Cu or Fe element, N is Avogadro's number. σ_{tot} is in unit of barn/atom. The photoelectric cross section σ_{ph} is obtained from σ_{tot} by subtracting the coherent and the incoherent scattering cross sections as interpolated from the tabulation value of Hubbell et al., [15][16] for Cu and Veigele [14] for Fe.

3. Results and Discussions

Mass attenuation coefficients of Cu and Fe measured at 41 characteristic line energies of 13 elements have been arranged in Table 1. Because of Si(Li) detector resolution has limited, only K_{α} , K_{β} lines are represented for Ti, V, Fe, Ni, Cu elementary targets. Utilizing Axil program of computer analysis for spectrum, K_{β_1} and K_{β_2} lines of Nb, Mo, Ag and Sn elementary targets were dissolved by Gaussian least-squares fit. The superimposed LX peaks of Au, Pb and I targets were dissolved into $L_{\alpha_1,2}$, $L_{\beta_1,2,3}$, L_{γ_1} , L_{γ_2} , L_{γ_3} and L_{γ_4} etc. lines and extracted (see Fig.3). The present experimental result of mass attenuation coefficient of Cu & Fe is shown in Table 1 and Fig.4, Fig.5. For comparison, the earlier experimental values are also shown in Fig.3, Fig.4. The solid line in Fig.4 or Fig.5 is the polynomial least-squares-fitted line with present results and only the uncertainties which are greater than $\pm 1\%$ have been shown by error bar.

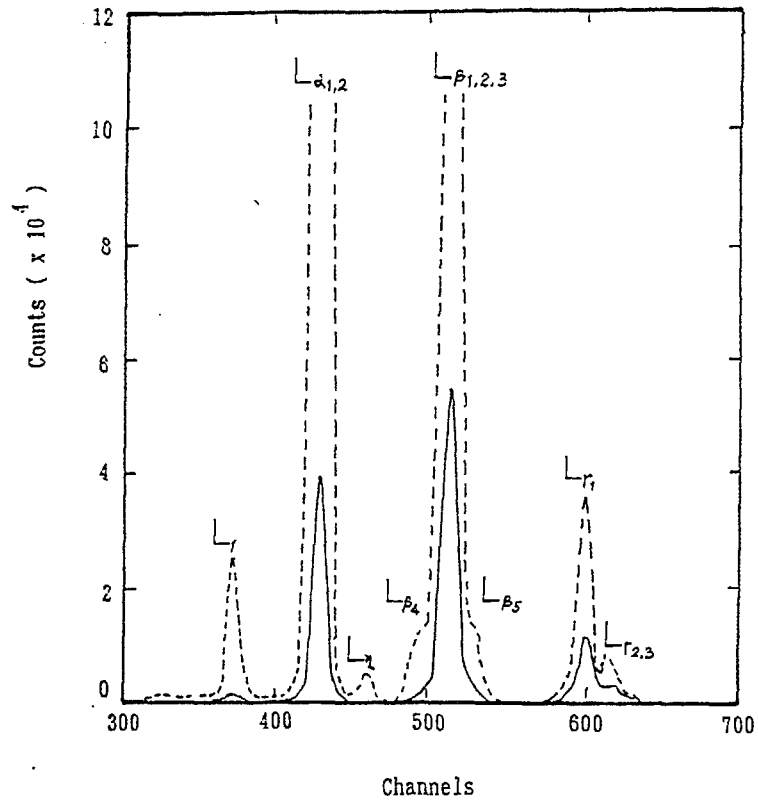


Fig. 3 X-ray spectrum from Pb target
bombarded with 2.5 MeV proton
--- with no Fe absorber
— with 18.77 mg/cm Fe absorber

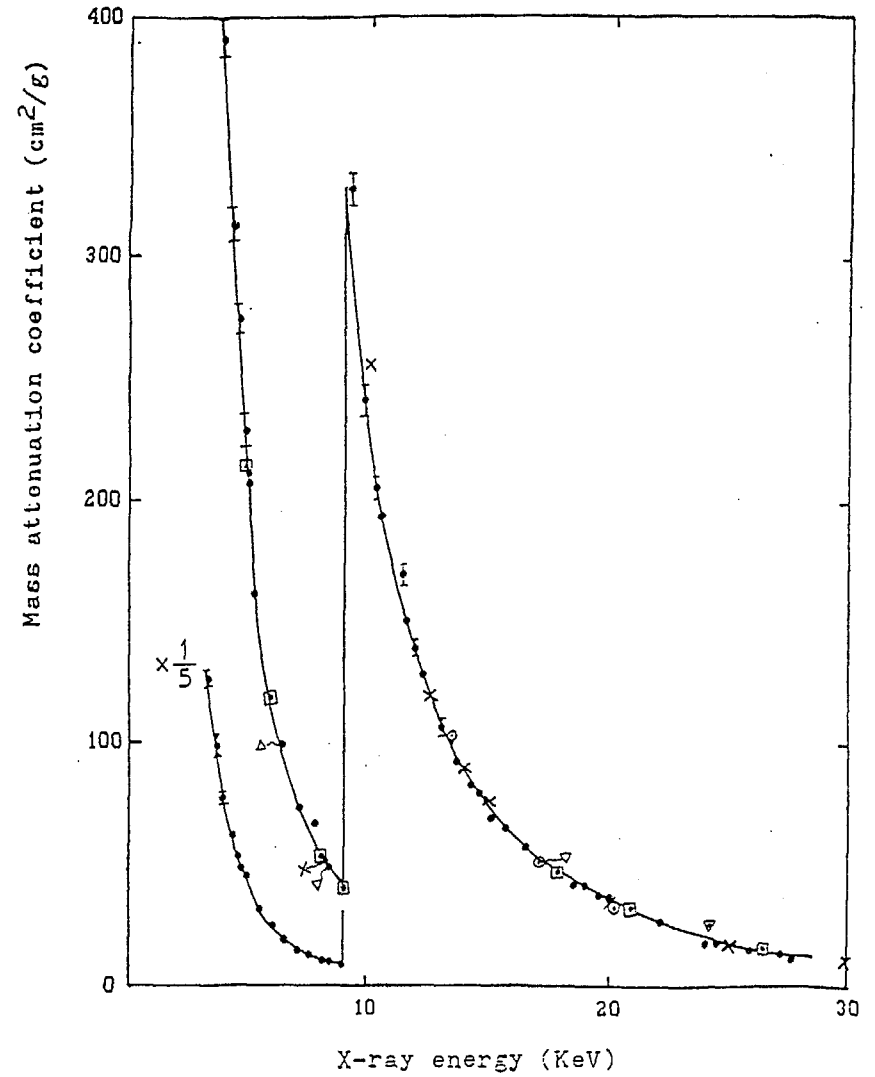


Fig. 4 Comparison of experimental results of mass
attenuation coefficient for Cu
● present work, □ [2], ▽ [3], × [4], △ [5], ○ [6]

TABLE 1. X-ray mass attenuation coefficients for Cu and Fe

Target	Characteristic line	Energy (KeV)	Attenuation coefficients (Cm ² /g)	
			Cu	Fe
Ti	K _α	4.509	267.0±2.7	195.4±1.9
	K _β	4.932	212.9±2.1	151.2±1.6
V	K _α	4.950	209.5±2.1	150.8±1.5
	K _β	5.427	159.4±1.6	118.5±1.2
Fe	K _α	6.399	99.8±1.0	69.1±0.7
	K _β	7.058	75.2±0.8	52.2±0.5
Ni	K _α	7.472	86.7±0.7	393.7±3.9
	K _β	8.265	50.2±0.5	297.8±3.0
Cu	K _α	8.041	53.7±0.5	322.0±3.2
	K _β	8.905	41.1±0.4	243.2±2.5
Nb	K _α	16.583	57.1±0.6	45.6±0.5
	K _{β₁₃}	18.617	41.8±0.4	32.8±0.5
	K _{β₂}	18.953	40.7±0.9	30.5±1.6
Mo	K _α	17.443	51.2±0.5	39.6±0.4
	K _{β₁₃}	19.602	36.9±0.4	28.3±0.3
	K _{β₂}	19.965	35.2±0.5	27.2±1.1
Ag	K _α	22.103	26.7±0.3	
	K _{β₁₃}	24.932	18.8±0.2	
	K _{β₂}	25.456	16.8±0.3	

TABLE 1. (Continue)

Target	Characteristic line	Energy (KeV)	Attenuation coefficients (cm ² /g)	
			Cu	Fe
Sn	K _α	25.192	18.3±0.2	
	K _{β₁₃}	28.472	13.7±0.2	
	K _{β₂}	29.109	13.2±0.2	
Au	L ₂	8.494	45.3±1.1	279 ±14
	L _{α₁₂}	9.707	242.6±6.1	196.1±2.0
	L _η	10.308	205.9±5.1	163.5±8.2
	L _{β₄}	11.205		139.5±7.0
	L _{β₁₂}	11.481		125.0±1.5
	L _{β₁₂₃}	11.484	151.3±1.5	
	L _{β₃}	11.610		121.0±9.6
	O ₅₄ - L ₃	11.916	130.6±2.0	
	L _{γ₁}	13.382	100.6±1.0	81.3±0.8
	L _{γ₂₃}	13.765	93.0±1.2	73.0±1.6
Pb	L ₂	9.185	329.9±7.0	229 ±11
	L _{α₁₂}	10.542	194.0±2.0	157.6±1.6
	L _η	11.349	171.8±5.3	128.0±7.7
	L _{β₁₂}	12.617		97.3±1.0
	L _{β₁₂₃}	12.621	119.2±1.2	
	L _{β₃}	12.793		94.0±13

TABLE 1. (Continue)

Target	Characteristic line	Energy (KeV)	Attenuation coefficients (cm ² /g)	
			Cu	Fe
Pb	L _{β₅}	13.015	107.3±1.6	
	L _{γ₁}	14.764	78.4±0.8	62.4±0.6
	L _{γ_{2,3}}	15.165	69.1±0.7	58.3±1.2
KI	K K _α	3.313	643.6±16.1	460 ±12
	K K _β	3.590	497.8±14.4	377 ±10
	I L _α	3.937	392.9±8.3	286 ± 8
	I L _{β_{1,3,4}}	4.251	315.5±6.6	232 ± 6
	I L _{β₂}	4.508	275.0±5.8	196 ± 5
	I L _{γ₁}	4.802	230.0±6.0	165 ± 4

The fitting of the X-ray mass attenuation coefficient for Cu and Fe were obtained by a third degree polynomial of the form:

$$Y=A_0+A_1 \cdot X+A_2 \cdot X^2+A_3 \cdot X^3 \quad (3)$$

for X-ray energies larger than the absorption edge and

$$Y=B_0+B_1 \cdot X+B_2 \cdot X^2+B_3 \cdot X^3 \quad (4)$$

for X-ray energies smaller than the absorption edge. where

$$Y=\ln \mu,$$

$$X=\ln E_x,$$

μ is the mass attenuation coefficient in unit of cm²/g, E_x is the x-ray energy in KeV. The fitting coefficients are as follows, for Cu

$$\begin{aligned} A_0 &= 0.219237 \text{ E}+02 \\ A_1 &= -0.134280 \text{ E}+02 \\ A_2 &= 0.368248 \text{ E}+01 \\ A_3 &= -0.416475 \text{ E}+00 \\ B_0 &= 0.862450 \text{ E}+01 \\ B_1 &= -0.597584 \text{ E}+00 \\ B_2 &= -0.133746 \text{ E}+01 \\ B_3 &= 0.266480 \text{ E}+00 \end{aligned}$$

for Fe

$$\begin{aligned} A_0 &= 0.683223 \text{ E}+01 \\ A_1 &= 0.253424 \text{ E}+01 \\ A_2 &= -0.196375 \text{ E}+01 \\ A_3 &= 0.241392 \text{ E}+00 \\ B_0 &= 0.960221 \text{ E}+01 \\ B_1 &= -0.330039 \text{ E}+01 \\ B_2 &= 0.550292 \text{ E}+00 \\ B_3 &= -0.174915 \text{ E}+00 \end{aligned}$$

The uncertainties for the attenuation experiment consisted of following terms: (1) The statistical uncertainty of count. (2) The error of measurement for absorption foil thickness and its uniformity. Both were less than ± 0.5%. (3) The uncertainty of computer dissolving spectrum and background. (4) the effect of scattering photon in solid angle subtended by detector. In our collimator condition the maximal scatter angle was less than 2°. The correction due to the scattering photon can be negligible. For the K_α, K_β, L_α, L_{β_{1,2,3}}, L_{γ₁} lines of each elementary target the statistical uncertainties of count and the uncertainties due to computer dissolving spectrum and background each and all were less than ± 0.5%. the total error of mass attenuation coefficients were set to be ± 1.0%. However for some weaker Lx lines the statistical uncertainties of count were somewhat greater ± 1% and for some superimposed LX peak, the uncertainty of computer dissolving spectrum was one of main error in the final result, the total error of mass attenuation coefficients were greater ± 1%. These data are also listed to Table 1 and Fig.4, Fig.5 for reference only.

The partial data have been compared with the earlier experimental results and shown in Table 2 and Table 3. It is obvious that there is a systematic deviation between the present results and the earlier results. the present results are systematically greater 2.6% than the earlier for both Cu and Fe. The data of Fe have also been compared with three tabulation values based on the earlier experimental results and shown in Table 4. There is a systematic deviation between Hubbell [17] and McMaster

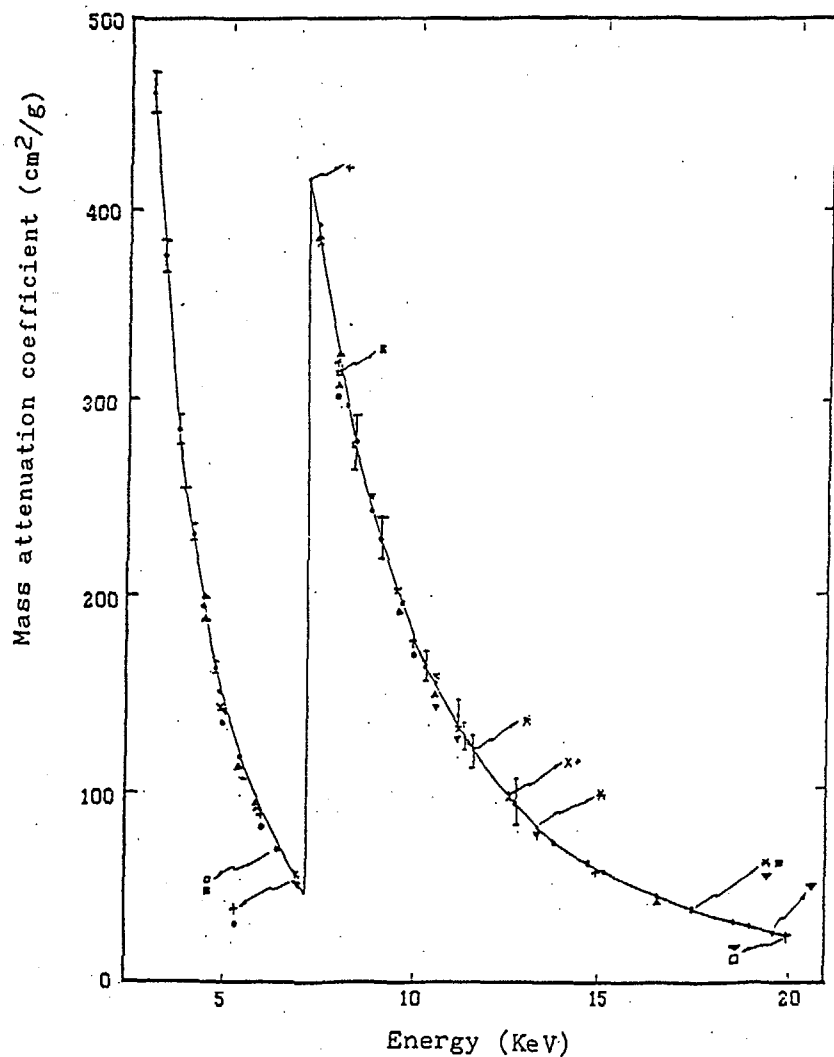


Fig.5 Comparison of experimental results of mass attenuation coefficient for Fe
 ● present work, ▲ [7], △ [8], □ [9],
 × [10], ▽ [11], ■ [12], * [13], + [14],

[18].Hubbell's tabulation values are systematically less (3-5.%) than the others. Present experimental results are higher than these tabulation data and close to the Veigele's values comparatively.

TABLE 2. Comparison of experimental results for Cu

X-ray energy (KeV)	Total attenuation cross section (in b/atom)					
	Present	MON[1]	PAR[2]	BAL[3]	BEA[4]	SH[5] RAN[6]
4.802	24270±633		23806±960			
4.932	22470±222	20619				
6.399	10533±105	10127				
6.4						10430±209
8.041	5664±57	5421	5700±110	5270±71		
8.048					5520±55	
8.905	4334±43	4096	4230±90			
10.542	20471±205	19932				
13.382	10615±105	10625				
13.432						10974±158
17.443	5402±54	5175		5176±71		
19.965	3717±53	3729			3530±35	
22.103	2820±28	2689		2646±23		
25.192	1933±20	1868				
28.472	1447±21	1312				

TABLE 3. Comparison of experimental results for Fe

X-ray (keV)	Mass attenuation coefficient (in cm²/g)					
	Present	Da[7]	Eh[8]	De[9]	Ca[10]	De[11] Co[12]
Ti k	4.509	195.4	187.8	200.4		
Fe k	7.058	52.2	52.4	52.2		
Cu K	8.041	322.0	308.3	326.6	310.0	306.1 314.3
Pb L	10.542	157.6	148.6		159.0	140.0

TABLE 4. Comparison of total attenuation cross sections for Fe with tabulation values (in b/atom)

Energy(keV)	Present	Vei[14]	Hub[17]	Mcma[18]
5.0	1.356 E+4	1.32 E+4	1.248 E+4	1.311 E+4
6.0	8.218 E+3	8.08 E+3	7.588 E+3	7.349 E+3
8.0	3.032 E+4	2.97 E+4	2.805 E+4	2.861 E+4
10.0	1.676 E+4	1.63 E+4	1.567 E+4	1.303 E+4
15.0	5.540 E+3	5.32 E+3	5.244 E+3	5.347 E+3
20.0	2.540 E+3	2.36 E+3	2.361 E+3	2.388 E+3

The total photoelectric cross sections, obtained by subtracting scattering cross section from the measured total cross sections, are compared with the theoretical compilations of Scofield [19] in Table 5. At X-ray energy range of 3 to 29 KeV photoeffect is a most essential interaction process. The total contribution of coherent and incoherent scattering is less than 3.5 % for Cu and less for Fe. The uncertainty of scattering cross section can not obviously influence the error of photoelectric cross sections. The present results of photoelectric cross section are greater than the theoretical values of Scofield [19] to 4.7 % for Cu and 5.1 % for Fe on an average.

As indicated above, theoretical calculations and some of earlier experimental data are lower than present results and the attenuation coefficient larger the deviation larger. The reason is obvious. At present measurement the dead time correction of Si(Li) system count was automatically done. Experiment measurement indicated that in spite of very small proton beam have been used, the difference of X ray intensities $I(t)$ without absorber foil and with maximal absorber thickness varied in two orders of magnitude. The dead time corrections were individually different. In our experimental condition the influence of these correction to the values was about 3 - 5 %. After correcting the value of μ became larger. In other hand, narrow - beam geometry for the measurement of X-ray attenuation coefficient was demanded that scattering photon entered Si(Li) detector as little as possible. The influence of scattering photon is not only concerned with

TABLE 5. Comparison of photoelectric cross sections (in b/atom) for Cu and Fe with theoretical values of Scofield [19]

Energy (KeV)	Present		Scofield		Deviation (%)	
	Cu	Fe	Cu	Fe	Cu	Fe
4.0	0.3956E+5		0.3629E+5		+9.0	
5.0	0.2102E+5	0.1334E+5	0.1973E+5	0.1274E+5	+6.5	+4.5
6.0	0.1246E+5	0.8005E+4	0.1192E+5	0.7671E+4	+4.5	+4.2
8.0	0.5526E+4	0.3014E+5	0.5341E+4	0.2819E+5	+3.5	+6.5
10.0	0.2421E+5	0.1665E+5	0.2263E+5	0.1571E+5	+7.0	+5.7
15.0	0.7668E+4	0.5486E+4	0.7711E+4	0.5215E+4	-0.2	+4.9
20.0	0.3596E+4	0.2439E+4	0.3491E+4	0.2323E+4	+3.0	+4.8

the dimension of narrow - beam geometry but also with the absorber thickness and the resolution of detector [20]. As increase of the absorber thickness the probability of scattering photon entering the Si(Li) detector increases so that the experimental data would deviate from the linear equation (1), as a result the fitted value of μ would decrease. At present the correlation coefficients of fitting linear equation (1) were greater than 0.9995. Even if the thickest absorber, the value of (μt) as big as 4.6, was used the experimental points did not deviate from the straight line yet. It indicated that in present experimental condition the influence of scattering photon to the final results can be neglected. Probably, these dead time corrections have not been done in some earlier measurements and it was a main reason why we obtained higher value of μ .

Using X rays produced by proton excitation of elementary targets and Si(Li) detector, the signal to noise ratio of characteristic X rays was promoted to 1 - 2 orders of magnitude in comparison with radioactive X - ray source or X - generator - secondary combination source. At the same time the error of dissolving spectrum was decreased. Experimental uncertainties of attenuation coefficients were reduced to ± 1 % for intense isolated X rays. Consequently, the results would be more confident and reliable.

REFERENCES

- [1] E. C. Montenegro et al.,
Atomic Data and Nucleat Data Tables Vol.22,131(1978)
- [2] K. Parthasaradhi and H. E. Hansen,
Phys.Rev. A Vol.10,563(1974)
- [3] T. O. Baldwin and F. N. Young JR.,
Phys.Rev. Vol. 163,591(1967)
- [4] A. J. Bearden, J.Appl. Phys. Vol. 37, 1681(1966)
- [5] Shahnawaz and Rao V. V., Curr. Sci. 46,256(1977)
- [6] Ram R. N. et al., Indian J. Phys. A 58,300(1984)
- [7] J. L. Dalton and J. Goldak ,
Can. Spectrosc, Vol.14, 171(1969)
- [8] C. E. Ehrenfried and D. E. Eodds,
AFSWC-TN-59-33(1960)
- [9] N. K. Del Grande et al. , UCRL-50174-SEC3(1969)
- [10] R. W. Carter et al. , Health Phys. , Vol.13, 593(1967)
- [11] R. D. Deslattes, AFOSR-TN-58-784(1958)
- [12] M. J. Cooper, Acta. Cryst. Vol.18, 813(1965)
- [13] L. H. Martin and K. C. Lang,
Proc. Roy. Soc.(London), Vol.137 A,199(1932)
- [14] WM. J. Veigele, Atomic Data, Vol.5, 51(1973)
- [15] J. H. Hubbell and I. Overbo,
J.Phys. Chem.Ref.Data. Vol.8,69(1979)
- [16] J. H. Hubbell et al.,
J. Phys. Chem. Ref. Data, Vol.5,471(1975)
- [17] J. H. Hubbell,
Int. J. Appl. Radiat. Isot. Vol.33, 1269(1982)
- [18] W. H. McMaster et al. , UCRL-50174 (1969)
- [19] J. H. Scofield, UCRL-51323 (1973)
- [20] K. M. Varier et al., Physical Review A33, 2378(1986)